CHEMISTRY OF MATERIALS

pubs.acs.org/cm

Article

Reactive Depolymerization of Polyethylene Terephthalate Textiles into Metal−Organic Framework Intermediates Produces Additive-Free Monomers

Published as part of Chemistry of Materials special issue "In Memory of Prof. Francis DiSalvo".

Abigail K. Nason, Wisarttra Phamonpon,[#] Tristan A. Pitt, Ronald T. Jerozal, Phillip J. Milner, Nadnudda Rodthongkum, and Jin Suntivich*

Cite This: https://doi.org/10.1021/acs.chemmater.4c02286

Read Online

ACCESS | Metrics & More | Article Recommendations | Supporting Information

ABSTRACT: Polyethylene terephthalate (PET) fibers can be transformed into a plethora of textile products by adding dyes, coatings, and trims. However, these additives make the chemical recycling of textile fibers challenging. The extraction of high-purity benzene-1,4-dicarboxylic acid (BDC), the major PET monomer from textiles, is, therefore, a major technical hurdle in textile circularity. Here, we demonstrate the extraction of high-quality BDC from PET fibers in textiles. Our approach uses reactive crystallization to turn PET directly into a metal−organic framework (MOF) using only metal salts and water as chemical inputs. Our process is base-free and organic-solvent-free. As BDC is the only component in this mixture capable of forming an extended, crystalline MOF network, the BDC monomers are separated from impurities as the MOF crystallizes. We demonstrate this concept on a post-consumer PET fabric, extracting colorless BDC monomers spectroscopically reminiscent of a virgin-grade material as the final product. Systematic control of the reaction parameters reveals the MOF assembly mechanism and the importance of the reaction conditions in promoting the metal-BDC complexation step prior to the MOF assembly.

INTRODUCTION

Textile global demand is rapidly increasing, with over 60 Mt produced in 2018 alone.[1,2] Polyethylene terephthalate (PET) is the most widely used textile material;[3,4] however, this class of materials is challenging to recycle.[5,6] Unlike bottles that can be recycled through melting and extrusion,[7] PET textiles are blended with dyes and additives.[8] Because these impurities can create undesired attributes in the final product, reusing PET from post-consumer textiles requires impurity separation. Chemical recycling or depolymerization of PET followed by purification offers a possible pathway; however, the purification step brings extra costs and complications.[9] Here, we present a strategy for integrating the depolymerization and purification steps into one using metal−organic frameworks (MOFs). We demonstrate that this approach can turn colored PET textiles into clean, colorless monomers spectroscopically reminiscent of petrochemically derived materials.

As one of the most widely used plastics, PET is a common polymer in textiles, packaging, and bottles.[10] PET fibers ("polyesters") are the largest category of PET and their use is rapidly growing. Therefore, the extraction of PET in post-consumer textiles plays a crucial role in the sustainability of PET manufacturing.[4] Palme et al. have demonstrated the recovery of PET monomers, benzene-1,4-dicarboxylic acid (BDC, also known as terephthalic acid), by using alkaline hydrolysis to depolymerize PET textiles.[11] However, several groups, including ours, have shown that dye impurities remained attached to the monomers.[12,13] Improvement in the purity of the monomers can be made through recrystallization, for example, by using organic solvents and chemical treatments. These approaches are, however, energy- and reagent-intensive, relying on nonaqueous solvents such as N,N-dimethylacetamide.[14] Pressurized water heating can take advantage of the increased BDC solubility; however, recrystallization without retrapping impurities or damaging the BDC is challenging.[15,16] Alternatively, one can use methanolysis to transform PET into dimethyl terephthalate (DMT) and take advantage of the DMT's lower melting point. This approach, however, requires additional methanol recovery and purification steps.[17]

We have previously shown that reactive crystallization can purify the BDC monomers and remove trapped dye impurities.

Received: August 14, 2024
Revised: September 24, 2024
Accepted: September 25, 2024

Our strategy takes advantage of the common usage of BDC as a constituent in MOFs,[18] a class of porous crystalline solids composed of metal-based secondary building units coordinated to multitopic organic ligands in a two- or three-dimensional ordered framework. We showed that BDC isolated from the alkaline hydrolysis of PET textiles can be purified using Ga^{3+} as the coordinating metal ion. This entirely aqueous-based process can return colorless BDC, reminiscent of virgin-grade materials. Nonetheless, our method requires several additional steps to facilitate the purification, including pretreatment of the polyester fabric with sodium hydroxide and sulfuric acid to recover the organic linker, BDC.

Driven to simplify the steps involved in recycling, we report an integrated process that combines depolymerization and reactive crystallization into one procedure. We are motivated to minimize the number of steps and remove the need to use base and acid as the depolymerization catalyst and pH adjuster, respectively. Valh et al. showed that PET textiles can be depolymerized directly under hydrothermal conditions; however, the base-acid purification steps were still needed to achieve a purity suitable for repolymerization.[19] Our process eliminates the need for a caustic, one of the cost factors in hydrolysis-based PET recycling,[20] by directly transforming PET plastics into MOFs, followed by a subsequent disassembly to monomers. We took inspiration from other works that synthesized MOFs directly from PET bottles, such as Cr-MOF, MIL-47(V), MIL-53(Cr), MIL-53(Al), MIL-53(Ga), and MIL-101(Cr) (MIL = Matériaux de l'Institut Lavoisier).[21−23] Unlike prior works, however, we have constrained our investigation to aqueous processing to avoid using organic solvents. We also focus on PET textiles instead of bottles, as the former contains significantly more impurities. We show that an extended network of Zn and terephthalate can be directly assembled from PET and disassembled into pure BDC monomers (Figure 1).

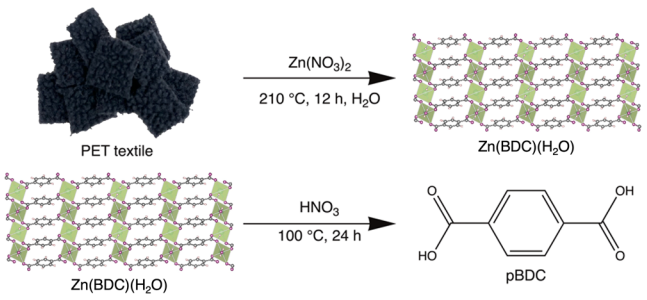

Figure 1. Schematic of the optimal procedure for recovering purified benzene-1,4-dicarboxylic acid (pBDC) from waste PET textiles. The PET textile is a black post-consumer fleece jacket made from polyethylene terephthalate (PET) plastic fibers.

Our approach starts by identifying reaction conditions that enable aqueous depolymerization and finding MOFs that can be formed in the same environment. We focus on metastable MOFs, with the rationale that their crystallization can be kinetically controlled but must not be too thermodynamically favorable to inhibit subsequent disassembly. Our first step is to select metal ions that can withstand the depolymerization condition and coordinate with BDC to assemble a metastable network. Through extensive literature research, we arrive at the metastable structures of the Zn-BDC MOF family. In this MOF family, synthesis conditions (e.g., time, pressure, temperature, and concentration) have been reported to drastically affect the obtained crystal structures and morphologies, even from the same reactants, revealing multiple competing forces in the self-assembly kinetics.[24] Researchers have used this phenomenon to create different metastable Zn-BDC MOFs by varying the reaction variables between Zn salts, BDC, and H_2O.[25,26] We leverage the Zn-BDC MOF metastability by transforming PET into Zn MOF intermediates, followed by a subsequent disassembly that turns Zn MOFs into the final purified BDC monomers.

EXPERIMENTAL METHODS

Reagents and Chemicals. Red polyester twill (100% polyester, pre-consumer) was purchased from Fabric Wholesale Direct. A post-consumer black polyester fleece was purchased from a secondhand clothing store (100% PET, as labeled by the tag). Both polyester textiles are assigned as 100% PET for mass-balance calculations and were used as received. Zinc nitrate hexahydrate ($Zn(NO_3)_2{\cdot}6H_2O$, Sigma-Aldrich, 98%), gallium(III) nitrate hydrate ($Ga(NO_3)_3{\cdot}xH_2O$, Beantown Chemical, 99.9%), aluminum nitrate nonahydrate ($Al(NO_3)_3{\cdot}9H_2O$, Sigma-Aldrich, ≥ 98%), aluminum chloride hexahydrate ($AlCl_3{\cdot}6H_2O$, Sigma-Aldrich, 99.9%), benzene-1,4-dicarboxylic acid (BDC, Sigma-Aldrich, 98%), acetone (Sigma-Aldrich, 99.9%), nitric acid (LabChem, 50% v/v), hydrochloric acid (HCl, Sigma-Aldrich, 37%), ethylene glycol (Sigma-Aldrich, 99.8%) and dimethyl sulfoxide (DMSO, Fisher chemical) were used as received. Deionized water was obtained from a water purification system (Millipore-Sigma, Direct-Q 5UV-R.)

Synthesis of MIL-53(Ga). We attempted to synthesize MIL-53(Ga) hydrothermally under autogenous pressure from PET fabric and BDC. For MIL-53(Ga) synthesis using PET, PET fabric (1 mmol, 0.192 g), $Ga(NO_3)_3{\cdot}xH_2O$ (1.07 mmol, 0.274 g), and 10 mL of deionized water were mixed in a 100 mL Teflon-lined autoclave, which was heated at 210 °C for 12 h. For MIL-53(Ga) synthesis using BDC, BDC (2.287 mmol, 0.38 g), $Ga(NO_3)_3{\cdot}xH_2O$ (1.917 mmol, 0.525 g), EG (2.287 mmol, 128 μL), and 10 mL of deionized water were mixed in a 100 mL Teflon-lined autoclave, which was heated at 210 °C for 5 h. This procedure was adapted from previous work.[12] The reaction mixtures were allowed to cool to room temperature and the solids were isolated via centrifugation. The resulting solid was rinsed with 40 mL deionized water and 10 mL acetone.

Synthesis of MIL-53(Al). The procedure was adapted from Loiseau et al.[27] MIL-53(Al)-NO_3 and MIL-53(Al)-Cl were hydrothermally synthesized under autogenous pressure separately using $Al(NO_3)_3{\cdot}9H_2O$ and $AlCl_3{\cdot}6H_2O$, respectively. PET fabric (5.188 mmol, 0.997 g), $Al(NO_3)_3{\cdot}9H_2O$ (5.188 mmol, 1.957 g) or $AlCl_3{\cdot}6H_2O$ (5.188 mmol, 1.253 g), and 30 mL of deionized water were mixed in a 100 mL Teflon-lined autoclave, which was heated to 210 °C for 12 h. The reaction mixture was allowed to cool to room temperature and the solids were isolated via centrifugation. The resulting solid was rinsed with 40 mL deionized water and 10 mL acetone. Then, the products were dried on a hot plate at 100 °C overnight before characterization.

Synthesis of Zn-BDC MOF Materials. A typical Zn-BDC MOF synthesis was performed as follows. Zn-BDC MOF was hydrothermally synthesized under autogenous pressure from a mixture of PET fabric (5.19 mmol, 0.997 g), $Zn(NO_3)_2{\cdot}6H_2O$ (5.19 mmol, 0.983 g), and 30 mL of deionized water. Our procedure was adapted from Yang et al.[28] The reactants were mixed in a 100 mL Teflon-lined autoclave before heating up to 210 °C for 12 h. The reaction mixture was allowed to cool to room temperature and the solids were isolated via centrifugation. The resulting solid was rinsed with 40 mL deionized water and 10 mL acetone. Then, the products were dried on a hot plate at 100 °C overnight before characterization.

Synthesis of Hydrothermal BDC (hBDC). hBDC was hydrothermally synthesized under autogenous pressure from a mixture of PET fabric (5.19 mmol, 0.997 g) and 30 mL of deionized water. The reactants were mixed in a 100 mL Teflon-lined autoclave before

https://doi.org/10.1021/acs.chemmater.4c02286
Chem. Mater. XXXX, XXX, XXX−XXX

heating up to 210 °C for 12 h. The reaction mixture was allowed to cool to room temperature and the solids were isolated via centrifugation. The resulting solid was rinsed with 40 mL deionized water and 10 mL acetone. Then, the products were dried on a hot plate at 100 °C overnight before characterization.

Decomposition of MIL-53(Al). MIL-53(Al) was disassembled by stirring the MOF with 7 molar equivalents of concentrated nitric acid. The mixture was stirred at 100 °C for 24 h in a lidded glass vial. After cooling the mixture to room temperature, the mixture was centrifuged five times with 10 mL deionized water per run to remove the remaining nitric acid and then once with 10 mL acetone. The product was dried on a hot plate at 100 °C overnight before characterization.

Decomposition of Zn-BDC MOF. Zn-BDC MOF was disassembled by stirring the MOF with 30 molar equivalents of concentrated nitric acid. The mixture was stirred at 100 °C for 24 h in a lidded glass vial. After cooling the mixture to room temperature, the mixture was centrifuged five times with 10 mL deionized water per run to remove the remaining nitric acid and then once with 10 mL acetone. The product was dried on a hot plate at 100 °C overnight before characterization. The yield of pBDC was 93% ± 2.84.

Characterization. The powder diffractometer (Bruker D8 Advance ECO) with a 1 kW Cu Kα source was used to collect powder X-ray diffraction (PXRD) patterns at a scanning rate of $0.02°s^{-1}$. All samples were dried overnight and ground with mortar and pestle before PXRD characterization. SEM images were collected on a Zeiss Gemini 500 scanning electron microscope. The samples were Au/Pd sputtered before imaging. The SEM was operated at an acceleration voltage of 3 kV with a working distance of 5.1 mm. UV−vis spectra (Shimadzu UV-2600i UV−vis spectrophotometer) were recorded in the 200−900 nm range. Blank DMSO was used as a background for all UV−vis experiments. UV−vis samples were run at 1 mM concentration in DMSO. Here, 0.1 mmol of each BDC sample was added to 10 mL DMSO and then diluted to 1 mM. XPS (Scienta Omicron ESCA-2SR) were analyzed at 10^{-9} Torr pressure. Monochromatic Al Kα X-rays (1486.6 eV) with photoelectrons were collected from a 1.1 mm diameter analysis spot. Photoelectrons were collected at a 90° emission angle and a 54.7° source-to-analyzer angle. A hemispherical analyzer determined electron kinetic energy, using a pass energy of 200 eV for wide/survey scans and 50 eV for high-resolution scans. A flood gun was used for charge neutralization of nonconductive samples. Colorimetric analysis was carried out by dissolving 5 mg of each BDC sample in glass vials of 2 mL DMSO. A change in the color of the solution was noted by observation. Thermogravimetric decomposition profiles were collected on a Q500 V6.7 thermogravimetric analyzer (TGA) using a temperature ramp of 3.00 °C/min from room temperature to 600.00 °C under an atmosphere of zero-grade air (20−22% O_2 in N_2). Data analysis was performed using the TRIOS software package. Attenuated total reflectance infrared (ATR-IR) spectra were collected on a Bruker Tensor II spectrometer equipped with a diamond ATR attachment. ^{1}H and ^{13}C NMR data were collected on a Bruker INOVA 500 MHz spectrometer in DMSO-d_6 solvent.

RESULTS AND DISCUSSION

We start by surveying a series of metal ions to determine which could directly turn PET into a MOF via reactive crystallization without needing to hydrolyze PET beforehand. We began with Ga^{3+}, which we had used in our previous work to transform impure BDC into MIL-53(Ga) MOF. Unfortunately, we observed no MIL-53(Ga) formation when combining the PET with $Ga(NO_3)_3{\cdot}xH_2O$. Irrespective of the hydrothermal conditions, we observed only BDC, which suggested that PET hydrolysis occurred but not MOF crystallization (see Supporting Information Figure S1a for PXRD). Given that we have previously observed MIL-53(Ga) assembly when subjecting recovered BDC to $Ga(NO_3)_3{\cdot}xH_2O$, we hypothesized that the presence of impurities in the sample hampered the MIL-53(Ga) formation. To validate that this observation is not due to the presence of ethylene glycol, the other monomer produced upon PET hydrolysis, we synthesized MIL-53(Ga) using BDC, $Ga(NO_3)_3{\cdot}xH_2O$, and ethylene glycol, following a literature procedure.[29] This experiment produced MIL-53(Ga), as supported by PXRD (see Supporting Information Figure S1b), suggesting that ethylene glycol is likely not the factor limiting MOF formation. Interestingly, Lo et al. found that the formation of MIL-53(Ga) could occur with HCl addition but not HF.[22] This finding suggests that the MIL-53(Ga) formation is sensitive to the presence of nonlinker additives. Given the uncontrolled nature of impurities in post-consumer textiles, we elected to find other MOFs to use for our depolymerization-crystallization process.

We next tested Al^{3+} due to the well-known hydrothermal synthesis of MIL-53(Al).[27] When treating PET with either $Al(NO_3)_3{\cdot}9H_2O$ or $AlCl_3{\cdot}6H_2O$ under hydrothermal conditions, we observed the successful formation of crystalline MIL-53(Al)-NO_3 and MIL-53(Al)-Cl, respectively (see Supporting Information Figure S2). However, we could not find a condition to disassemble the obtained MIL-53(Al) back to BDC using acid. We hypothesize that, based on the hard and soft acid and base theory,[30] high valence Al^{3+} (a hard Lewis acid) binds strongly to the carboxylate linker BDC^{2-} (a hard Lewis base), making MIL-53(Al) highly stable.[31] Using excessive temperature and time causes the reaction to form insoluble precipitates, such as AlOOH (boehmite), as shown by the postdrying PXRD[32,33] (see Supporting Information Figure S3.)

It became evident that the ideal coordinating metal should not bind to BDC so strongly that disassembly requires harsh conditions and inevitable side reactions, as was the case with Al^{3+}. We hypothesized that Zn^{2+}, a lower valence and borderline hard/soft Lewis acid known for its ability to coordinate with BDC to form water-sensitive MOFs such as MOF-5[34] and MOF-2,[35] would work well for this purpose. Several papers have shown that these MOFs transform into different crystalline phases when exposed to water.[36,37] For example, MOF-5 ($Zn_4O(BDC)_3$) undergoes phase transitions at water concentrations higher than 0.6 mol/L.[38] Similarly, MOF-2 ($[Zn(BDC)(H_2O)]{\cdot}DMF$) undergoes a structural transition to a different crystalline zinc phase, $Zn(BDC)(H_2O)_2$, when it is humidified.[39] The extreme sensitivity of Zn-MOFs makes the solvent selection, whether aqueous or nonaqueous, the choice of the anions, and other crystallization conditions essential in controlling the interaction between Zn^{2+} and BDC.[40−42] We hypothesized that synthesizing a Zn-BDC MOF using water instead of an organic solvent could directly make these crystalline phases, allowing for a greener synthesis route. Another advantage of Zn^{2+} over most other metal cations is its relatively low cost and high abundance.

To synthesize Zn-MOF from PET, a mixture of red PET fabric, $Zn(NO_3)_2{\cdot}6H_2O$, and water was heated in a Teflon-lined autoclave at 210 °C for 12 h. The PXRD pattern of the prepared $Zn(BDC)(H_2O)$ MOF (Figure 2) matches well with the literature,[39] confirming that impure PET fabric can serve as the organic linker source in the synthesis. The resulting MOF contained BDC linkers, as confirmed by PXRD.

We tested various molar ratios of Zn:BDC and reaction times to determine the effect of synthesis conditions on MOF formation (Figure 3). Previous studies have shown that Zn-MOFs can be synthesized with water as a solvent using a 1:1:2 molar mixture of Zn:BDC:NaOH in a hydrothermal reaction vessel.[28,41] We adapted our procedure from these conditions

https://doi.org/10.1021/acs.chemmater.4c02286
Chem. Mater. XXXX, XXX, XXX−XXX

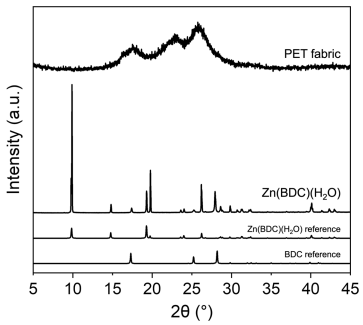

Figure 2. Powder X-ray diffraction of the PET fabric precursor (top) and $Zn(BDC)(H_2O)$ MOF synthesized from red PET fabric under the conditions of 2:1 Zn:BDC, 210 °C, and 12 h (bottom). The simulated PXRD pattern of each known phase based on single-crystal XRD analysis is included for reference.

but omitted the NaOH to eliminate the use of a caustic base, a drawback of most PET hydrolysis systems. A mixture of $Zn(NO_3)_2{\cdot}6H_2O$, PET textile, and water in a mol ratio of 1:1:320 was reacted hydrothermally. Through PXRD analysis and Pawley refinement of the data (see Supporting Information Figures S4−S17), we observed successful depolymerization and partial assembly of PET into a crystalline network at reaction times of 6 h and greater (Figure 3b). After 6 h, new reflections are observed with the most intense peaks at 2θ = 9.8, 14.7, and 19.8°, matching $Zn(BDC)(H_2O)$.[28,39,41] At 18 h, there is growth of an intermediate structure $Zn(BDC)(H_2O)_2$ with the most intense peaks at 2θ = 12.2 and 16.9°. At 24 h, both $Zn(BDC)(H_2O)_2$ and $Zn(BDC)(H_2O)$ are present, as well as an unknown phase termed unknown structure 1 with a peak at 2θ = 11 and 19.8°. The structure of unknown 1 could not be solved using single-crystal XRD. However, we propose a structural formula of Zn(BDC) based on the TGA analysis (see Supporting Information Table S2 and Figure S19). At 48 h, $Zn(BDC)(H_2O)_2$ disappears and the proportion of unknown structure 1 (Zn(BDC)) in the mixture grows significantly, based on visual comparison. At 72h, unknown structure 1 (Zn(BDC)) is the only phase identified, aside from the unreacted linker. The presence of the unknown structure 1 (Zn(BDC)) at long reaction times leads us to believe that this is the thermodynamically stable structure. The PXRDs at all reaction times show characteristic peaks of BDC at 2θ = 17.3, 25.2, and 27.9°, in varying degrees, indicating that a molar ratio of 1:1 Zn:BDC is not enough to coordinate all of the generated BDC.

Recognizing that a 1:1 Zn:BDC ratio was insufficient to coordinate all the BDC, we doubled the molar ratio of Zn to BDC (2:1). At the shortest reaction time of 4 h, there were only PXRD peaks for BDC and PET present (Figure 4a). At 6 h, we started to observe MOF formation; however, both PXRD and SEM images showed that BDC and PET were still the dominant solids (see Supporting Information Figure S20). The first MOF formed at 6 h, $Zn(BDC)(H_2O)$, was not a stable phase as the reaction time was extended. At 24 h and using a 2:1 Zn:BDC ratio, multiple structures are present, including unknown structure 1 (Zn(BDC)), $Zn(BDC)(H_2O)_2$, and a new phase, $Zn_2(OH)_2(BDC)(H_2O)$, with the most intense peaks at 2θ = 8.8 and 17.6°. At 48 and 72 h, there is further transition to this new structure, $Zn_2(OH)_2(BDC)(H_2O)$. This structure, along with $Zn(BDC)(H_2O)$, persisted at 72 h of reaction time. When doubling the Zn:BDC ratio again to 4:1, we saw a complete conversion of the Zn-MOF to $Zn_2(OH)_2(BDC)(H_2O)$ after 6 h, suggesting that the subsequent conversion from $Zn(BDC)(H_2O)$ to $Zn_2(OH)_2(BDC)(H_2O)$ is facilitated by excess Zn^{2+} in solution, which limited its formation at lower ratios of Zn:BDC. We graphically represent how the reaction stoichiometries and times affect the crystal phase in a phase diagram in Figure 3a.

As the reaction time increases, the intensities of BDC reflections decrease compared to the MOF peaks. Our observation suggests that the Zn-MOF formation occurs only after PET hydrolysis begins and a critical BDC concentration is reached. To start, the Zn^{2+} ions likely catalyze the hydrolysis of PET fibers by weakening the PET-water interface and

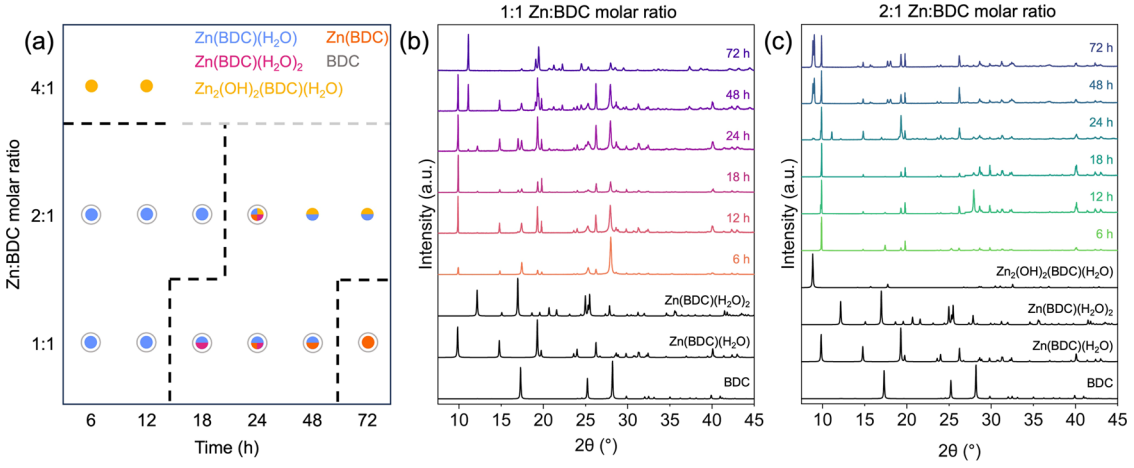

Figure 3. (a) Kinetic phase diagram showing the effect of Zn:BDC molar ratio and reaction time on the synthesized Zn-MOF structure. The gray rings represent unreacted BDC as detected by PXRD. Black dashed lines represent phase transitions. Gray dashed line represents predicted phase transition. (b) Time-course PXRD changes of 1:1 Zn:BDC molar ratio MOF syntheses with increasing reaction time. (c) Time-course PXRD changes of 2:1 Zn:BDC molar ratio MOF syntheses with increasing reaction time. $Zn(BDC)(H_2O)$, $Zn(BDC)(H_2O)_2$, and $Zn_2(OH)_2(BDC)(H_2O)$ structures have been confirmed by PXRD with Pawley Refinements that can be found in Supporting Information Figures S4−S17. Zn(BDC) structure was unable to be resolved by Pawley Refinements. We propose this structure based on the TGA analysis and ATR-IR (See Supporting Information Figures S19 and S26).

https://doi.org/10.1021/acs.chemmater.4c02286
Chem. Mater. XXXX, XXX, XXX−XXX

increasing the rate of hydrolysis.[43] Additionally, the Lewis acidity of Zn^{2+} may contribute to the catalytic activity in the hydrolysis reaction. Zn^{2+}, a Lewis acid, can coordinate with the carbonyl oxygen of the ester group in the PET polymer backbone. This coordination polarizes the carbonyl bond, making the carbonyl carbon more electrophilic and susceptible to nucleophilic attack by a water molecule. The Brønsted acidity of the hydrated zinc complex[44] adds to the catalytic activity by protonating the ester oxygen of the PET backbone. This protonation further increases the electrophilicity of the carbonyl carbon, facilitating the nucleophilic attack by a water molecule. Together, these two acidities enhance the overall catalytic efficiency of Zn^{2+} in the hydrolysis of PET. This depolymerization step deposits BDC on the PET surface (the modified shrinking core model[45]). The SEM images taken at 6 h showed the fibers exhibited rough surfaces in contrast to smooth pristine PET fibers, likely due to BDC deposition (see Supporting Information Figure S20). The BDC then coordinates the Zn^{2+} ions to form Zn-MOFs,[23] freeing the surface for additional PET hydrolysis. The cycle continues until the PET hydrolysis is completed.

To gain better mechanistic insight into MOF formation, we used pristine, commercial BDC to synthesize Zn-MOFs in place of the PET fabric. Using identical conditions, we heated a mixture of commercial BDC, $Zn(NO_3)_2{\cdot}6H_2O$, and water (2:1:320) at 210 °C for various times. Under these conditions, we found no formation of Zn-MOF at all the tested reaction times (Figure 4b). When adding ethylene glycol, however, we observed the Zn-MOF formation (see Supporting Information Figure S21). We thus conclude that the EG released from PET hydrolysis plays a crucial role in MOF formation. We have identified two hypotheses to explain this. First, it is well-known that EG can dissolve large amounts of multivalent-ion salts, including Zn^{2+}, effectively increasing the Zn^{2+} concentration in solution.[46,47] In addition, BDC has a higher solubility in EG than water, increasing the BDC solubility in the reaction mixture.[48] Although Zn^{2+} is not saturated in the reaction mixture and is easily soluble in water, we believe the EG is providing a mutual solvent for both Zn^{2+} and BDC, allowing for the reaction to proceed. Alternatively, at early reaction times, Zn^{2+} and EG might complex to form an insoluble coordination polymer of zinc glycolate (Zn-(OCH_2CH_2O)).[49,50] This polymer could provide a nucleation site or intermediate for Zn-MOF formation. Combining both observations, we hypothesize that the Zn-MOF synthesis proceeds via an EG-assisted solvation of Zn ions and soluble BDC in the liquid phase.

Putting these observations together, we propose the following formation mechanism of Zn-BDC MOFs from PET and $Zn(NO_3)_2{\cdot}6H_2O$. The first step is the depolymerization of PET into BDC and EG, catalyzed by Zn^{2+}. Detection of BDC in PXRD in several samples indicates that the BDC crystallizes and precipitates from the reaction mixture. Then, the presence of EG increases the solubility of BDC and Zn^{2+}, allowing for the coordination of BDC to Zn ions in the solution. As the Zn-MOFs form, the solution runs out of BDC and Zn, causing additional BDC and Zn to dissolve. The observed initial Zn-BDC MOF phase, $Zn(BDC)(H_2O)$, likely results from the first kinetic product crystallized out of solution under these conditions.

The experiments above were conducted with pre-consumer polyester twill; we next investigated whether Zn-MOFs assembled from post-consumer PET fabric can purify BDC.

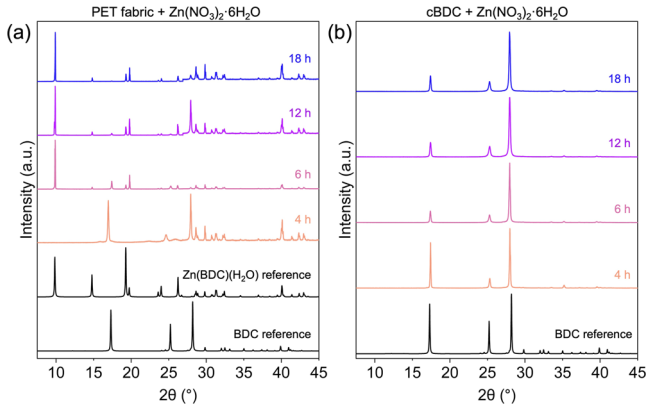

Figure 4. Powder X-ray diffractions showing the products formed at different reaction times when using (a) PET fabric and (b) commercial BDC (cBDC) as the organic linker source and $Zn(NO_3)_2{\cdot}6H_2O$ as the metal salt in a 2:1 molar ratio at 210 °C. The PXRDs in (a) at 6, 12, and 18 h showing the structure $Zn(BDC)(H_2O)$ have corresponding Pawley refinements in Supporting Information Figures S10–S12. The 4 h, 2:1 Zn:BDC PXRD shows BDC and unreacted PET fabric.

Using a post-consumer fleece made of PET (black color), we mixed the PET textile, $Zn(NO_3)_2{\cdot}6H_2O$, and water in a 1:1:320 molar ratio and heated at 210 °C for 12 h. PXRD of the prepared Zn-MOF (Supporting Information Figure S22) matches well the $Zn(BDC)(H_2O)$ features reported in the literature mixed with unreacted BDC.[39] The yield of $Zn(BDC)(H_2O)$ is 65% with respect to both Zn^{2+} and PET. As discussed above, Zn-MOF formation is limited by the amount of free Zn^{2+}. The presence of unreacted BDC was, therefore, expected given the 1:1 Zn:BDC molar ratio. Our goal here is not necessarily to convert all PET to Zn-MOF but to demonstrate the recovery of clean BDC using minimal input chemicals (Figure 5). The MOF/BDC suspension was centrifuged to separate the solid, pale-yellow MOF and BDC from the bright yellow supernatant solution. The supernatant solution likely consists largely of dyes and other additives. SEM showed that the obtained particles were on the order of 1–10 μm with rectangular crystallite features (see Supporting Information Figure S23). The MOF/BDC solid was subsequently rinsed with water to wash off any remaining remnants of impurities and with acetone to assist in drying.

Having demonstrated that a mixture of Zn-MOF and BDC can be obtained directly from post-consumer plastics, we next disassembled the Zn-MOF by heating it in nitric acid. This process yields purified BDC (pBDC), which precipitated as a solid from an aqueous solution of $Zn(NO_3)_2$. Complete Zn-MOF to BDC conversion was found to occur at an equivalent 30:1 molar ratio of HNO_3:BDC at 100 °C for 24 h with stirring. The yield of pBDC was 93% ± 2.84. The PXRD of the disassembled product shows the characteristic BDC peaks at 2θ = 17.21, 25.01, and 27.64° (Figure 5b). ^1H and ^{13}C NMR also confirm the presence of BDC (see Supporting Information Figure S24). We assessed the purity of the pBDC sample dissolved in DMSO using UV–vis spectroscopy by comparing it against commercial BDC and BDC produced directly from hydrothermal hydrolysis of PET fleece fabric at 210 °C for 12 h (hBDC) (Figure 5d). Comparing the absorbance spectra of pBDC to commercial BDC, both have the characteristic UV-absorbance features of BDC with no other absorbance features. hBDC, on the other hand, exhibits additional absorbance

https://doi.org/10.1021/acs.chemmater.4c02286
Chem. Mater. XXXX, XXX, XXX–XXX

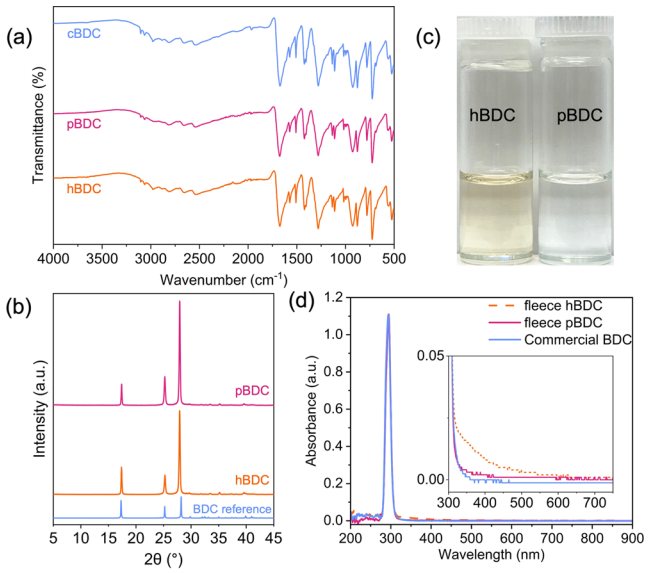

Figure 5. (a) Attenuated total reflectance infrared (ATR-IR) spectra of commercial BDC (cBDC), purified BDC (pBDC) made from the disassembly of 1:1 Zn:BDC 12 h Zn(BDC)(H_2O) MOF, and hydrothermal BDC (hBDC) made from the hydrothermal hydrolysis of black fleece post-consumer PET fabric. (b) Powder X-ray diffraction of pBDC and hBDC. (c) Photos and (d) UV−vis spectra of hBDC and pBDC in DMSO.

between 350−500 nm, indicating the presence of impurities such as dyes. These impurities can also be seen as a yellow hue in the solution in the photo in Figure 5c. pBDC was further tested for Zn impurities using X-ray photoelectron spectroscopy (XPS). This test showed Zn impurities of less than 0.01 atomic percent (referenced against carbon and oxygen, Supporting Information Figure S25). This observation suggests that pBDC has a purity close to the commercial BDC monomers, validating our hypothesis that we could use a cycle of Zn-MOF assembly−disassembly to turn PET into impurity-free BDC monomers.

CONCLUSIONS

We report a one-step depolymerization-crystallization of post-consumer PET textiles using a Zn-BDC MOF as an intermediate. We demonstrated the recovery of purified BDC, a PET monomer, following the acid-induced Zn-MOF disassembly, without needing base addition. The formation of Zn-BDC MOFs greatly depended upon reaction conditions. We attributed this sensitivity to the MOF assembly mechanism, which for Zn-BDC MOF, requires BDC to dissolve and coordinate with Zn^{2+} ions. Owing to the need for the solution-phase complexation pathway, adjusting the Zn:BDC molar ratio and reaction time significantly affected the final Zn-BDC MOF crystal structures. We also found that PET cannot react directly with Zn ions to form Zn-BDC MOF. Instead, the PET must first undergo hydrolysis to create BDC. Only when BDC is present in solution can the MOF begin to form. The transformation cycle thus cascades through PET hydrolysis, BDC deposition-precipitation, BDC dissolution, Zn-BDC complexation, and Zn-MOF formation. In the case of PET, the presence of byproduct ethylene glycol, the other monomer of PET, likely helps promote the synthesis by increasing the solubility of Zn^{2+} and BDC in the solvent. Our work demonstrates the environmental sensitivity of reactive crystallization and how understanding it could advance the separation science critical to sustainability.

ASSOCIATED CONTENT

Supporting Information

The Supporting Information is available free of charge at https://pubs.acs.org/doi/10.1021/acs.chemmater.4c02286.

Additional XRD, TGA, NMR, FTIR, SEM, and XPS characterization (PDF)

AUTHOR INFORMATION

Corresponding Author

Jin Suntivich − *Department of Materials Science and Engineering and Kavli Institute for Nanoscale Science, Cornell University, Ithaca, New York 14853, United States;* orcid.org/0000-0002-3427-4363; Email: jsuntivich@cornell.edu

Authors

Abigail K. Nason − *Department of Materials Science and Engineering, Cornell University, Ithaca, New York 14853, United States;* orcid.org/0000-0002-3424-8886

Wisarttra Phamonpon − *Department of Materials Science and Engineering, Cornell University, Ithaca, New York 14853, United States; Nanoscience and Technology Program, Graduate School, Chulalongkorn University, Bangkok 10330, Thailand*

Tristan A. Pitt − *Department of Chemistry and Chemical Biology, Cornell University, Ithaca, New York 14853, United States*

Ronald T. Jerozal − *Department of Chemistry and Chemical Biology, Cornell University, Ithaca, New York 14853, United States*

Phillip J. Milner − *Department of Chemistry and Chemical Biology, Cornell University, Ithaca, New York 14853, United States;* orcid.org/0000-0002-2618-013X

Nadnudda Rodthongkum − *Metallurgy and Materials Science Research Institute, Chulalongkorn University, Bangkok 10330, Thailand;* orcid.org/0000-0002-0379-5166

Complete contact information is available at: https://pubs.acs.org/10.1021/acs.chemmater.4c02286

Author Contributions

#W.P. is a co-first author. The manuscript was written through contributions of all authors. All authors have given approval to the final version of the manuscript. Author contributions have been described using CRediT taxonomy. A.K.N.: methodology, investigation, validation, visualization, writing−original draft, writing−review and editing. W.P.: investigation, validation, visualization, writing−original draft. T.A.P.: formal analysis, visualization, writing−review and editing. R.T.J.: investigation. P.J.M.: funding acquisition, project administration, resources, supervision, writing−review and editing. N.R.: funding acquisition, supervision. J.S.: conceptualization, funding acquisition, methodology, resources, project administration, supervision, visualization, writing−original draft, writing−review and editing. A.K.N. and W.P. performed MOF synthesis and disassembly, PXRD, and SEM experiments. T.A.P. performed Pawley Refinements, ATR-IR, and TGA experiments. R.T.J. performed UV−vis spectroscopy experiments. A.K.N., W.P., and J.S. wrote the original draft with inputs from all authors.

https://doi.org/10.1021/acs.chemmater.4c02286
Chem. Mater. XXXX, XXX, XXX−XXX

Notes

The authors declare no competing financial interest.

■ ACKNOWLEDGMENTS

This material is based upon work supported by the National Science Foundation under Grant No. CHE-2155157 for alkaline reactivity studies (J.S.) and No. CBET-2047627 for MOF synthesis and characterization (T.A.P., R.T.J., P.J.M.). A.K.N. acknowledges the National Science Foundation Graduate Research Fellowship under Grant No. DGE-1650441 and DGE-2139899. This work made use of the Cornell Center for Materials Research Shared Facilities which are supported through the NSF MRSEC program (DMR-1719875). Any opinions, findings, and conclusions or recommendations expressed in this material are those of the author(s) and do not necessarily reflect the views of the National Science Foundation. We also acknowledge the support of a Camille Dreyfus Teacher-Scholar Award to P.J.M. (TC-23-048). W.P., N.R., and J.S. are grateful for the Global Strategic Collaboration Award between Cornell University and Chulalongkorn University.

■ REFERENCES

(1) Zhang, L.; Leung, M. Y.; Boriskina, S.; Tao, X. Advancing Life Cycle Sustainability of Textiles through Technological Innovations. *Nat. Sustain* **2023**, *6* (3), 243−253.
(2) Niinimäki, K.; Peters, G.; Dahlbo, H.; Perry, P.; Rissanen, T.; Gwilt, A. The Environmental Price of Fast Fashion. *Nat. Rev. Earth Environ* **2020**, *1* (4), 189−200.
(3) Park, S. H.; Kim, S. H. Poly (Ethylene Terephthalate) Recycling for High Value Added Textiles. *Fashion and Textiles* **2014**, *1* (1), 1.
(4) *Materials Market Report 2023*. Textile Exchange. https://textileexchange.org/knowledge-center/documents/materials-market-report-2023/ (accessed 2024-01-02).
(5) Zamani, B.; Svanström, M.; Peters, G.; Rydberg, T. A Carbon Footprint of Textile Recycling: A Case Study in Sweden. *Journal of Industrial Ecology* **2015**, *19* (4), 676−687.
(6) Wang, S.; Salmon, S. Progress toward Circularity of Polyester and Cotton Textiles. *Sustainable Chemistry* **2022**, *3* (3), 376−403.
(7) Shen, L.; Worrell, E.; Patel, M. K. Open-Loop Recycling: A LCA Case Study of PET Bottle-to-Fibre Recycling. *Resources, Conservation and Recycling* **2010**, *55* (1), 34−52.
(8) MacArthur, E. *A New Textiles Economy: Redesigning Fashion's Future*; Ellen MacArthur Foundation, 2017, pp. 1−150.
(9) Ügdüler, S.; Geem, K. M. V.; Denolf, R.; Roosen, M.; Mys, N.; Ragaert, K.; Meester, S. D. Towards Closed-Loop Recycling of Multilayer and Coloured PET Plastic Waste by Alkaline Hydrolysis. *Green Chem.* **2020**, *22* (16), 5376−5394.
(10) Spychaj, T. Chemical Recycling of PET: Methods and Products. In *Handbook of Thermoplastic Polyesters*; John Wiley & Sons, Ltd, 2002; pp. 1252−1290.
(11) Palme, A.; Peterson, A.; de la Motte, H.; Theliander, H.; Brelid, H. Development of an Efficient Route for Combined Recycling of PET and Cotton from Mixed Fabrics. *Textiles and Clothing Sustainability* **2017**, *3* (1), 4.
(12) Nason, A. K.; Jerozal, R. T.; Milner, P. J.; Suntivich, J. Reactive Crystallization via Metal−Organic-Framework Formation Enables Separation of Terephthalic Acid from Textile Impurities. *ACS Sustainable Chem. Eng.* **2023**, *11* (1), 18−22.
(13) Li, Y.; Yi, H.; Li, M.; Ge, M.; Yao, D. Synchronous Degradation and Decolorization of Colored Poly(Ethylene Terephthalate) Fabrics for the Synthesis of High Purity Terephthalic Acid. *Journal of Cleaner Production* **2022**, *366*, No. 132985.
(14) Wu, S.-C.; Cheng, Z.-M.; Wang, S.-D.; Shan, X.-L. Recovery of Terephthalic Acid from Alkali Reduction Wastewater by Cooling Crystallization. *Chem. Eng. Technol.* **2011**, *34* (10), 1614−1618.
(15) Myerson, A. S.; Gaines, S. THE AGGLOMERATION AND AGING OF TEREPHTHALIC ACID PARTICLES IN LIQUID SOLUTION. *Particulate Science and Technology* **1983**, *1*, 409.
(16) Dunn, J. B.; Burns, M. L.; Hunter, S. E.; Savage, P. E. Hydrothermal Stability of Aromatic Carboxylic Acids. *Journal of Supercritical Fluids* **2003**, *27* (3), 263−274.
(17) Sinha, V.; Patel, M. R.; Patel, J. V. Pet Waste Management by Chemical Recycling: A Review. *J. Polym. Environ* **2010**, *18* (1), 8−25.
(18) Furukawa, H.; Cordova, K. E.; O'Keeffe, M.; Yaghi, O. M. The Chemistry and Applications of Metal-Organic Frameworks. *Science* **2013**, *341* (6149), 1230444.
(19) Valh, J. V.; Vončina, B.; Lobnik, A.; Zemljič, L. F.; Škodič, L.; Vajnhandl, S. Conversion of Polyethylene Terephthalate to High-Quality Terephthalic Acid by Hydrothermal Hydrolysis: The Study of Process Parameters. *Text. Res. J.* **2020**, *90* (13−14), 1446−1461.
(20) Cornell, D. D. Recycling Polyesters by Chemical Depolymerization. In *Modern Polyesters: Chemistry and Technology of Polyesters and Copolyesters*; John Wiley & Sons, Ltd, 2004; pp. 563−590.
(21) Ren, J.; Dyosiba, X.; Musyoka, N. M.; Langmi, H. W.; North, B. C.; Mathe, M.; Onyango, M. S. Green Synthesis of Chromium-Based Metal-Organic Framework (Cr-MOF) from Waste Polyethylene Terephthalate (PET) Bottles for Hydrogen Storage Applications. *Int. J. Hydrogen Energy* **2016**, *41* (40), 18141−18146.
(22) Lo, S.-H.; Raja, D. S.; Chen, C.-W.; Kang, Y.-H.; Chen, J.-J.; Lin, C.-H. Waste Polyethylene Terephthalate (PET) Materials as Sustainable Precursors for the Synthesis of Nanoporous MOFs, MIL-47, MIL-53(Cr, Al, Ga) and MIL-101(Cr). *Dalton Trans.* **2016**, *45* (23), 9565−9573.
(23) Deleu, R. W. P.; Stassen, I.; Jonckheere, D.; Ameloot, R.; Vos, D. E. D. Waste PET (Bottles) as a Resource or Substrate for MOF Synthesis. *J. Mater. Chem. A* **2016**, *4* (24), 9519−9525.
(24) Clausen, H. F.; Poulsen, R. D.; Bond, A. D.; Chevallier, M.-A. S.; Iversen, B. B. Solvothermal Synthesis of New Metal Organic Framework Structures in the Zinc−Terephthalic Acid−Dimethyl Formamide System. *J. Solid State Chem.* **2005**, *178* (11), 3342−3351.
(25) Leroy, C.; Métro, T.-X.; Hung, I.; Gan, Z.; Gervais, C.; Laurencin, D. From Operando Raman Mechanochemistry to "NMR Crystallography": Understanding the Structures and Interconversion of Zn-Terephthalate Networks Using Selective 17O-Labeling. *Chem. Mater.* **2022**, *34* (5), 2292−2312.
(26) Carton, A.; Abdelouhab, S.; Renaudin, G.; Rabu, P.; François, M. Structure of Zinc Hydroxy-Terephthalate: Zn3(OH)4(C8H4O4). *Solid State Sci.* **2006**, *8* (8), 958−963.
(27) Loiseau, T.; Serre, C.; Huguenard, C.; Fink, G.; Taulelle, F.; Henry, M.; Bataille, T.; Férey, G. A Rationale for the Large Breathing of the Porous Aluminum Terephthalate (MIL-53) Upon Hydration. *Chem.−A Eur. J.* **2004**, *10* (6), 1373−1382.
(28) Yang, S.-Y.; Long, L.-S.; Huang, R.-B.; Zheng, L.-S. Crystal structure of a 3D coordination polymer: zincterephthalate hydrate. *Main Group Metal Chem.* **2002**, *25* (5), 329−330.
(29) Volkringer, C.; Loiseau, T.; Guillou, N.; Férey, G.; Elkaïm, E.; Vimont, A. XRD and IR Structural Investigations of a Particular Breathing Effect in the MOF-Type Gallium Terephthalate MIL-53(Ga). *Dalton Trans.* **2009**, *12*, 2241−2249.
(30) Pearson, R. G. Hard and Soft Acids and Bases. *Journal of the American Chemical society* **1963**, *85* (22), 3533−3539.
(31) Qian, X.; Yadian, B.; Wu, R.; Long, Y.; Zhou, K.; Zhu, B.; Huang, Y. Structure Stability of Metal-Organic Framework MIL-53 (Al) in Aqueous Solutions. *Int. J. Hydrogen Energy* **2013**, *38* (36), 16710−16715.
(32) Leus, K.; Bogaerts, T.; De Decker, J.; Depauw, H.; Hendrickx, K.; Vrielinck, H.; Van Speybroeck, V.; Van Der Voort, P. Systematic Study of the Chemical and Hydrothermal Stability of Selected "Stable" Metal Organic Frameworks. *Microporous Mesoporous Mater.* **2016**, *226*, 110−116.
(33) Bezverkhyy, I.; Ortiz, G.; Chaplais, G.; Marichal, C.; Weber, G.; Bellat, J.-P. MIL-53(Al) under Reflux in Water: Formation of γ-AlO(OH) Shell and H2BDC Molecules Intercalated into the Pores. *Microporous Mesoporous Mater.* **2014**, *183*, 156−161.

https://doi.org/10.1021/acs.chemmater.4c02286
Chem. Mater. XXXX, XXX, XXX−XXX

(34) Eddaoudi, M.; Kim, J.; Rosi, N.; Vodak, D.; Wachter, J.; O'Keeffe, M.; Yaghi, O. M. Systematic Design of Pore Size and Functionality in Isoreticular MOFs and Their Application in Methane Storage. *Science* **2002**, *295* (5554), 469−472.
(35) Li, H.; Eddaoudi, M.; Groy, T. L.; Yaghi, O. M. Establishing Microporosity in Open Metal−Organic Frameworks: Gas Sorption Isotherms for Zn(BDC) (BDC = 1,4-Benzenedicarboxylate). *J. Am. Chem. Soc.* **1998**, *120* (33), 8571−8572.
(36) Huang, L.; Wang, H.; Chen, J.; Wang, Z.; Sun, J.; Zhao, D.; Yan, Y. Synthesis, Morphology Control, and Properties of Porous Metal−Organic Coordination Polymers. *Microporous Mesoporous Mater.* **2003**, *58* (2), 105−114.
(37) Kaye, S. S.; Dailly, A.; Yaghi, O. M.; Long, J. R. Impact of Preparation and Handling on the Hydrogen Storage Properties of Zn4O(1,4-Benzenedicarboxylate)3 (MOF-5). *J. Am. Chem. Soc.* **2007**, *129* (46), 14176−14177.
(38) Hausdorf, S.; Wagler, J.; Mo*β*ig, R.; Mertens, F. O. R. L. Proton and Water Activity-Controlled Structure Formation in Zinc Carboxylate-Based Metal Organic Frameworks. *J. Phys. Chem. A* **2008**, *112* (33), 7567−7576.
(39) Edgar, M.; Mitchell, R.; Slawin, A. M. Z.; Lightfoot, P.; Wright, P. A. Solid-State Transformations of Zinc 1,4-Benzenedicarboxylates Mediated by Hydrogen-Bond-Forming Molecules. *Chem.−A Eur. J.* **2001**, *7* (23), 5168−5175.
(40) Getachew, N.; Chebude, Y.; Diaz, I.; Sanchez-Sanchez, M. Room Temperature Synthesis of Metal Organic Framework MOF-2. *J. Porous Mater.* **2014**, *21* (5), 769−773.
(41) Thirumurugan, A.; Rao, C. N. R. 1,2-, 1,3- and 1,4-Benzenedicarboxylates of Cd and Zn of Different Dimensionalities: Process of Formation of the Three-Dimensional Structure. *J. Mater. Chem.* **2005**, *15* (35−36), 3852−3858.
(42) Guilera, G.; Steed, J. W. Topological Control in Coordination Polymers by Non-Covalent Forces. *Chem. Commun.* **1999**, *16*, 1563−1564.
(43) Campanelli, J. R.; Cooper, D. G.; Kamal, M. R. Catalyzed Hydrolysis of Polyethylene Terephthalate Melts. *J. Appl. Polym. Sci.* **1994**, *53* (8), 985−991.
(44) Migliorati, V.; Mancini, G.; Tatoli, S.; Zitolo, A.; Filipponi, A.; De Panfilis, S.; Di Cicco, A.; D'Angelo, P. Hydration Properties of the Zn2+ Ion in Water at High Pressure. *Inorg. Chem.* **2013**, *52* (2), 1141−1150.
(45) Yoshioka, T.; Okayama, N.; Okuwaki, A. Kinetics of Hydrolysis of PET Powder in Nitric Acid by a Modified Shrinking-Core Model. *Ind. Eng. Chem. Res.* **1998**, *37* (2), 336−340.
(46) Knetsch, D.; Groeneveld, L. W. Alcohol as Ligands. III. Complexes of Ethylene Glycol with Some Divalent Metal Halides. *Inorg. Chim. Acta* **1973**, *7*, 81−87.
(47) Abbott, A. P.; Barron, J. C.; Ryder, K. S.; Wilson, D. Eutectic-Based Ionic Liquids with Metal-Containing Anions and Cations. *Chemistry−A. European Journal* **2007**, *13* (22), 6495−6501.
(48) Larrañaga, M. D.; Lewis, R. J.; Lewis, R. A. *T-Hawley's Condensed Chemical Dictionary*, 16th ed.; John Wiley & Sons, Ltd, 2016; pp. 1300−1396.
(49) Das, J.; Evans, I. R.; Khushalani, D. Zinc Glycolate: A Precursor to ZnO. *Inorg. Chem.* **2009**, *48* (8), 3508−3510.
(50) Krasil'nikov, V. N.; Tyutyunnik, A. P.; Zhukov, V. P.; Baklanova, I. V.; Gyrdasova, O. I.; Chulkov, E. V. Zinc Glycolate Zn(OCH2CH2O): Synthesis and Structure, Spectral and Optical Properties, Electronic Structure and Chemical Bonding. *J. Alloys Compd.* **2022**, *924*, No. 166320.

https://doi.org/10.1021/acs.chemmater.4c02286
Chem. Mater. XXXX, XXX, XXX−XXX